TRR
JOURNAL OF THE TRANSPORTATION RESEARCH BOARD

Research Article

Transportation Research Record
1–15

DOI: 10.1177/03611981251394677
journals.sagepub.com/home/trr
Sage

Research on Engine Braking Force and Critical Slope Length Based on Truck Power-to-Weight Ratio

Dibin Wei[1], Chi Zhang[1], Yanyang Gao[1], Tingyu Guo[1], and Bo Wang[1]

Abstract

Addressing the current issue of inadequate safety on continuous longitudinal slopes of mountain highways caused by "vehicles not adapting to the road," this paper constructs a model for calculating engine braking force and critical downhill slope length from the truck's power-to-weight ratio perspective. First, the energy conversion process during the truck's long downhill journey is analyzed based on energy conservation, and a suitable brake drum temperature rise model is selected and calibrated using real vehicle test data. Through simulation, the relationship between braking torque and rated engine power is quantified, and the mathematical model's validity is confirmed by comparing the simulation results with model calculations. Finally, the downhill engine braking process for trucks is analyzed, and the quantitative relationship between speed and distance for trucks with varying power-to-weight ratios is determined using differential equations. By integrating the mainstream power-to-weight ratios of Chinese trucks and reasonable deceleration rates, a model for the vehicle speed and critical slope length of 5–8 kW/t power-to-weight ratio vehicles on 1%–12% longitudinal slopes is derived. The results of this research contribute to ensuring the braking safety of trucks with different weight ratios during continuous long downhill travel and provide a reference for establishing reasonable design indexes.

Keywords

power-to-weight ratio, engine braking, conservation of energy, semi-articulated train, critical slope length

At the end of 2023, the total mileage of China's highways reached 5.4368 million kilometers, an increase of 82,000 km from the end of 2022, and the highway density reached 56.63 km/100 km^2 (*1*). The generalized mountainous area in China accounts for two-thirds of the land area (*2*). The risk of traffic accidents in continuous long downhill sections of mountainous highways is relatively high, and the reason is usually truck brake failure (*3*, *4*). With the development of mountain highway construction in China, the safety of the continuous longitudinal slopes of mountain highways must be improved (*5*). It is significant to carry out theoretical research on the longitudinal slope design of mountainous highways to reduce traffic accidents caused by road factors.

Scientifically and reasonably controlling the gradient and length of highway vertical slopes is one of the fundamental methods to reduce traffic accidents. Implementing effective safety measures for downhill sections is paramount when constrained by terrain conditions. In this regard, many studies have emphasized the importance of reasonably controlling vertical slope gradients for enhancing road safety (*6*, *7*). Furthermore, recent research has deepened our understanding of braking-distance formation and brake-system behavior under varied operating conditions. Advanced analytical frameworks incorporating multibody dynamics and nonlinear mechanics have been developed to better estimate braking distance (*8*). The impact of weather conditions on braking performance has also received considerable attention, with studies demonstrating how friction degradation caused by rain, snow, and ice significantly extends

[1]School of Highway, Chang'an University, Xi'an, China

Corresponding Author:
Chi Zhang, zhangchi@chd.edu.cn

braking distance across different vehicle categories (*9*). Several studies have also investigated brake thermal failure to ensure the safe operation of trucks. Ultimately, brake temperature rise models have been established from multiple perspectives, including the mechanical equilibrium of truck downhill movement, traffic accidents on descending slopes, and real vehicle testing (*10–12*).To address brake thermal failure risks in heavy vehicles, research has focused on accurate evaluation of thermal loads on brake drums under severe service conditions, revealing the risk of material property loss at high temperatures and providing foundation for further finite-element analyses (*13*). In addition, some studies have also found an interaction between traffic flow characteristics, such as vehicle speed and slope length. Based on this, the relationship between slope and slope length under different traffic flow characteristics has been studied (*14*). Moreover, several coupled factors have been taken into consideration. For instance, researchers have examined the interaction between combined horizontal and vertical alignments, leading to the development of a mountain road safety model (*15*). Additionally, significant efforts have been made to establish a comprehensive analytical model for accident causation specifically in long downhill tunnels of mountain expressways (*16*).

The adaptation between vehicle performance characteristics and vertical slope design parameters plays a pivotal role in determining road safety. In the case of trucks, the power-to-weight ratio emerges as a fundamental factor affecting the uphill velocity of large commercial vehicles. It is an essential consideration in designing dedicated truck climbing lanes (*17*). With the continuous advancement of automotive engineering, vehicle performance has been progressively enhanced, leading to potential incompatibilities between the capabilities of mainstream vehicle models and the specifications outlined in contemporary standards or manuals (*18*, *19*). Therefore, it is crucial to investigate the performance of trucks with varying power-to-weight ratios on vertical slope alignments, particularly in speed characteristics, acceleration capabilities, and safety performance (*20–23*). However, it is important to note that most studies have only investigated the relationship between the power-to-weight ratio and the uphill climbing performance of trucks, calculating the critical slope length for uphill directions, while lacking consideration of the impact of truck continuous braking performance on vertical alignment indicators for different grades of highways in downhill scenarios.

In recent years, engine power has increased significantly. However, research on the mainstream truck power-to-weight ratio and sustained braking performance is insufficient, as it usually focuses only on a single power-to-weight ratio model derivation. It is essential to study the relationship between the power-to-weight ratio and the performance of the vehicle's continuous braking device to determine the speed changes when these vehicles experience sustained braking force while traveling downhill and to develop a reasonable critical slope length.

Given the above limitations, this paper innovatively combines the energy conservation and temperature rise model, based on continuous long downhill real-vehicle tests, systematically for the mainstream power-to-weight ratio of trucks, using the law of conservation of energy to construct mathematical models and simulation experiments to quantify the performance of engine braking performance, and studies the trend of truck movement on long downhill slopes. Designers can more accurately formulate design schemes for trucks with different power-to-weight ratios, which not only helps to improve road traffic efficiency, but also effectively guarantees the braking safety of trucks on continuous long downhill sections, and provides a reliable basis for formulating scientific design indicators and optimizing speed limit measures.

The remainder of this paper is structured as follows. The next section presents the construction process of the theoretical model, encompassing the analysis of energy conversion principles and the calibration of the brake temperature rise model, followed by a section detailing the experiment procedure of the simulation study, including parameter configuration and analysis of simulation data. The section after that demonstrates the methodology for determining critical slope length, incorporating theoretical analysis of average vertical slope and the computation of critical slope length. In the penultimate section, we discuss the implications of the research findings for the design and management of continuous longitudinal slopes in mountainous areas, analyze the limitations of this study, and identify potential directions for future research. In the final section, we conclude the study and present its potential benefits for road traffic safety.

Theoretical Model

Analysis of Energy Conversion

The value of the change in gravitational potential energy, ΔE_p, is converted into other energy as the truck travels from the top of the slope to the bottom of the slope at a constant speed. Figure 1 shows the schematic diagram of energy conversion.

In Figure 1, the exhaust brake and the engine brake do not exist at the same time. The exhaust brake is opened by the driver's control, and this study considers the most unfavorable engine braking for further analysis. Retarder braking requires trucks to be equipped with an additional hydraulic or eddy current retarder.

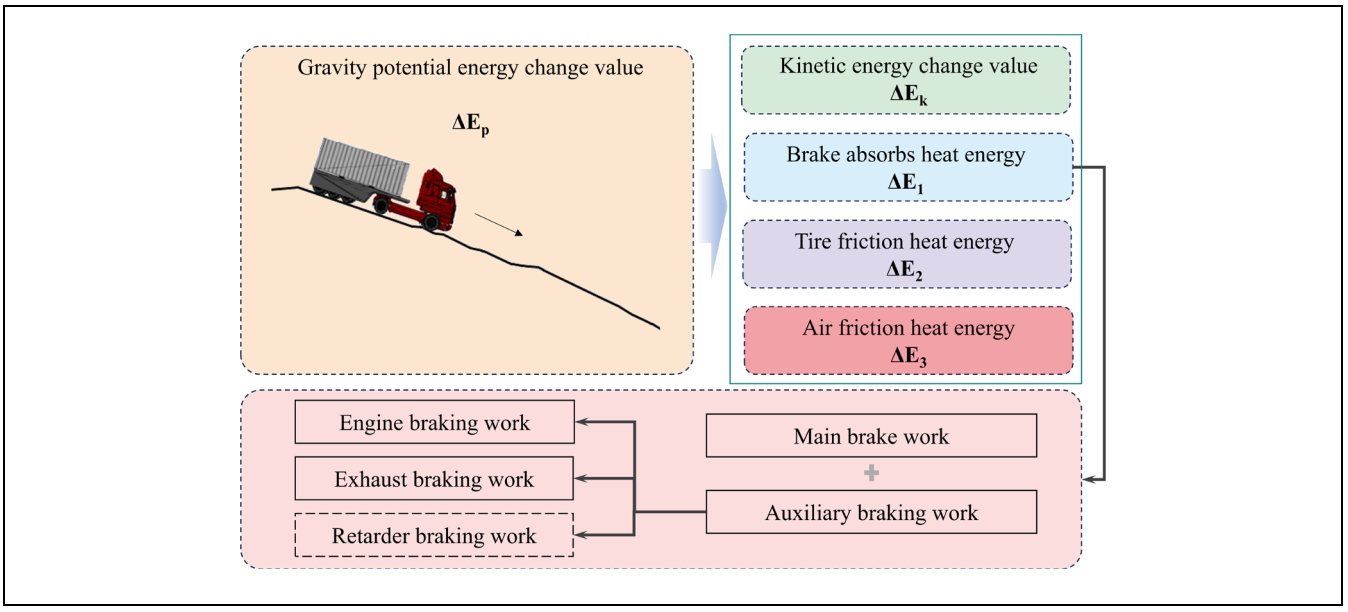

Figure 1. Truck downhill energy conversion diagram.

Given the current situation in China, where the installation rate of such auxiliary systems remains extremely low, this study does not include retarder braking in the energy conversion analysis. This assumption aligns with a conservative modeling principle aimed at evaluating the highest braking demand on the engine and service brake.

However, it is important to note that in markets where retarder systems are widely adopted, the braking energy would be distributed more significantly to the retarder, thereby reducing the load on both the engine and service braking systems. In these contexts, the energy balance and performance characteristics may differ and warrant separate modeling consideration. Therefore, in this study, the change in potential energy during braking is primarily reflected in the work performed by the main brake and the engine brake, under the assumption of no auxiliary braking intervention.

Engine braking occurs when the engine stops fueling, the clutch is engaged, and the transmission is not in neutral gear. The high-speed vehicle will drag the running engine, making it similar to an air compressor that consumes the truck's kinetic energy to slow down. This mechanism allows the engine to act as a consumer of the truck's kinetic energy, thereby achieving a braking effect. The engine braking work is eventually converted into heat energy, and the energy will be discharged with the exhaust gas and lost to the atmosphere through the exhaust system. The work of the main brake is mainly converted into energy in the main brake, and the heat is radiated to the surrounding space.

Based on the assumption that the kinetic energy change value ΔE_k of the whole vehicle is zero when it goes downhill at a constant speed, the work done by the truck when the engine brakes when it goes downhill is calculated according to Equation 1.

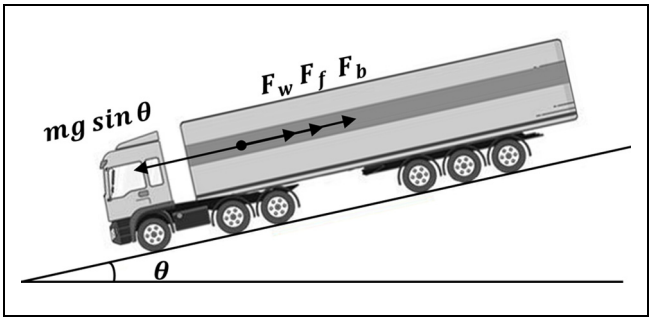

Figure 2. Dynamic analysis of truck operation.

$$W_e = \Delta E_p - \Delta E_2 - \Delta E_3 - E_g - Q_{out} \quad (1)$$

where

W_e = the work done by the engine brake,
E_g = internal energy stored in the brake drum, and
Q_{out} = the convective heat of thermal convection between the brake drum and the external air.

Non-Braking Force Impact Analysis. When the truck runs at a constant speed during the downhill driving with a slope length of L and a constant slope of θ, its mechanical balance on the slope is as shown in Figure 2.

The truck is subjected to gravity along the ramp component $mg \sin \theta$, air resistance F_w, road rolling resistance

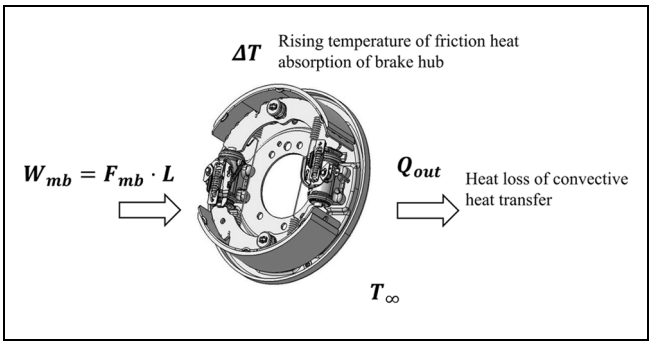

Figure 3. Energy analysis of brake drum.

F_f, and vehicle braking force F_b; the relationship is as Equation 2. The non-braking force of the truck during the downhill process includes rolling resistance and air resistance.

$$mg\sin\theta = F_w + F_f + F_b \tag{2}$$

Usually, the calculation of the rolling resistance F_f is equal to the product of the rolling resistance coefficient and the wheel load. The calculation of heat generated by rolling resistance is shown in Equation 3. The rolling resistance coefficient of truck tires on good roads can be calculated by Equation 4 (*24*).

$$\Delta E_2 = F_f \cdot L = f \cdot mgL\cos\theta \tag{3}$$

$$f = 0.0076 + 0.000056V \tag{4}$$

where
L = the rolling distance (m), and
V = the vehicle speed (km/h).

The air resistance is the component of the air force in the driving direction when the vehicle is moving downhill in a straight line. When analyzing the air resistance, the influence of the lateral force and yaw moment generated by the air resistance on the longitudinal driving of the vehicle is not considered. The heat generated by air resistance is shown in Equation 5.

$$\Delta E_3 = F_w \cdot L = \frac{1}{2}CSL\rho u^2 \tag{5}$$

where
C = the air resistance coefficient,
ρ = the air density (kg/m^3),
S = the windward area (m^2), and
u = the relative speed (the driving speed of the vehicle when there is no wind) (m/s).

Braking Force Impact Analysis. The energy conversion problem of the brake drum is discussed as a whole without considering the energy loss caused by its own wear. Assuming that the truck only uses the most unfavorable working condition of engine braking downhill, it can be considered that the vehicle braking force is divided into two parts (*25*). In Equation 6, the braking force F_b is composed of the braking force F_{mb} of the main brake and the braking force F_{eb} of the engine.

$$\Delta E_1 = F_b L = (F_{mb} + F_{eb})L \tag{6}$$

According to the above analysis, when the main brake of the vehicle is working, the negative work done by the main brake during the downhill process is converted into internal energy stored in the brake drum and heat energy lost in the air (*26*). The heat generated by the friction between the drum and the brake shoes is absorbed by the drum and increases the temperature ΔT. At the same time, considering the thermal convection between the drum and the external air, the drum dissipates heat to the outside world. The convective heat is Q_{out}, and the energy conversion is as shown in Figure 3.

The negative work done by the main brake on the vehicle is converted into internal energy stored in the brake drum and heat energy lost in the air, as shown in Equation 7. The internal energy E_g stored in the brake drum is calculated by Equation 8.

$$W_{mb} = F_{mb}L = E_g + Q_{out} \tag{7}$$

$$E_g = nc_g m_g \Delta T \tag{8}$$

where
n = the number of brake drums,
c_g = the specific heat capacity of the brake drum,
m_g = the mass of the brake drum, and
ΔT = the temperature change value.

There are three forms of heat transfer: heat conduction, heat convection, and heat radiation. The contact area between the brake drum and the surrounding solid is small, and the thermal resistance is large. Therefore, it is considered that the heat of thermal heat transfer can be ignored (*27*). Secondly, the radiation heat dissipation generally accounts for 5%–10% of the heat dissipation, and its proportion decreases with the decrease of the brake drum temperature. In contrast, the convective heat dissipation accounts for more than 80% of the total heat dissipation. Therefore, in the calculation of the heat dissipation of the brake drum, heat conduction and heat radiation are usually ignored, and the convection heat dissipation on the outer surface is the main factor. The calculation method of convective heat transfer Q_{out} and convective heat transfer coefficient h can be seen in Equations 9 and 10.

$$Q_{out} = nhA(T - T_\infty) \cdot \frac{L}{V} \tag{9}$$

Table 1. Experiment Section Information

Road section	Starting pile number	Ending pile number	Average slope (%)	Cumulative slope length (km)	Relative height difference (m)	Continuous downhill section spacing (km)
①	ZK81 + 930	ZK63 + 700	−2.06	18.23	436.983	11.148
②	ZK52 + 510	ZK33 + 545	−2.40	18.97	384.01	

$$h = 5.224 + 1.55Ve^{-2.778 \times 10^{-3}} \tag{10}$$

where

h = the convective heat transfer coefficient of the brake drum (W/(m^2·K)),
T_∞ = the ambient temperature (°C), and
A = the outer surface area of the brake drum (m^2).

Theoretical Model Construction. Calculating the temperature value in E_g and Q_{out} is a complex problem. In the past few years, scholars have produced many research results on the brake drum temperature rise model. At present, the modeling methods of braking temperature rise can be divided into the theoretical analysis method, the measured regression method, and the software simulation method (*28*). This paper selects a representative temperature rise model that aligns with the development trend of China's freight transport (*29*). The model introduces the critical longitudinal slope, considering the heating and cooling of the brake drum under different slope conditions. When the longitudinal slope is greater than the critical longitudinal slope, the main brake and the auxiliary brake are required to work together, which is the heating process. When the slope is less than the critical longitudinal slope, the auxiliary brake can complete the braking process on its own, which is the cooling process. The specific model is as follows:

$$\begin{aligned} &i \leqslant i_0 : T = (T_0 - T_\infty)e^{\frac{-h_c AL}{m_d c_d V}} + T_\infty \\ &i > i_0 : T = (T_0 - \frac{0.95V(\beta F_s r_d - N_a - N_h) + T_\infty h_c A}{7.2 r_t h_c A})e^{\frac{-h_c AL}{m_d c_d V}} \\ &\quad + \frac{0.95V(\beta F_s r_d - N_a - N_h) + T_\infty h_c A}{7.2 r_t h_c A} \end{aligned} \tag{11}$$

where

T_0 = the initial temperature (°C),
T_∞ = the ambient temperature (°C),
i_0 = the critical longitudinal slope (%) under engine braking,
L = the slope length (m),
V = the vehicle speed (m/s),
F_s = the ground braking force on the wheel,
r_d = the tire power radius (m),
r_t = the tire rolling radius (m),
β = the braking force distribution coefficient,
N_a = the braking torque generated by the engine braking,
N_h = the tire hysteresis torque,
h_c = the convective heat transfer coefficient,
A = the outer surface area of the brake drum (m^2),
m_d = the mass of the brake drum (kg), and
c_d = the specific heat capacity of the brake drum (J/(kg·°C)).

The heat generated by the main braking force can be calculated through the above temperature rise model. When the truck goes downhill at a constant speed, the negative work done by the engine braking force W_e is equal to the product of the engine braking force F_{eb} and the distance acting on the vehicle L, as shown in Equation 12. According to Equations 1, 2, 3, 5, 6, 7, 8, 9, and 12, Equation 13 can be derived.

$$W_e = F_{eb}L \tag{12}$$

$$\begin{aligned} F_{eb} = mg(\sin\theta - f\cos\theta) - \frac{1}{2}C\rho SV^2 \\ - \frac{n}{L}[c_g m_g \Delta T + hA(T - T_\infty)] \end{aligned} \tag{13}$$

Equation 13 can solve the engine braking force according to the energy conservation equation. Since the temperature calculation module in the model is related to the parameters of the vehicle and the road, it is necessary to use real vehicle test data to calibrate the temperature rise model before using it to predict the temperature of the brake drum, to ensure that the model has a better prediction effect.

Model Calibrating

Real Vehicle Data Acquisition. The Kangding-Ya'an section of the G4218 Ya'an-Yecheng expressway in the southwest mountainous area of China was selected as the research section to carry out real vehicle tests. The expressway is located in the transition zone from the western plain of the Sichuan Basin to the Qinghai-Tibet Plateau. The altitude difference of the whole line is as high as more than 1,800 m, which is a typical long and continuous longitudinal slope section.

The real vehicle test was conducted on carefully selected test sections with relevant parameters, which are shown in Table 1. Multiple continuous downhill tests

Table 2. Test Vehicle Parameters

Unit	Content	Parameter
Complete vehicle	Model number	ZZ4257W324HE1B
	Complete vehicle mass (kg)	8,800
	Maximum allowable traction mass (kg)	40,000
Engine	Model number	MC13.54-50
	Rated power (kW)	397
	Maximum torque (N·m)	2,500
	Maximum speed ($km \cdot h^{-1}$)	101
Gear box	Model number	HW25712XSTCL
	Transmission ratio of each gear	14.941/11.611/8.986/6.987/5.514/4.318/3.460/2.689/2.081/1.618/1.277/1.000
	Main transmission ratio	4.11
	Efficiency of transmission	0.8
Tire	Tire rolling radius (mm)	537.7

were performed using a typical six-axle semi-trailer truck. Articulated trains now constitute over 51% of freight models and account for more than 80% of total highway freight turnover in 2022. Accordingly, we selected a China Heavy Duty Truck HOWO T7 as the test vehicle, with a full-load mass limited to 49 tons (detailed parameters in Table 2). The test sections featured clean, flat road surfaces with minimal traffic, and tests were escorted by road administration vehicles to minimize traffic interference. All tests were conducted under favorable weather conditions, actively avoiding extreme weather events. After each test, data were backed up and equipment functionality was thoroughly verified before proceeding.

A total of four drivers with more than 10 years of driving experience and familiarity with the road conditions were involved in this test. Before the test, information was communicated to the driver about the driving operation that needed to be undertaken. Combined with the relevant literature, it is found that similar real vehicle brake drum temperature test experiments mostly use double or more even-numbered tests to ensure the richness of test data (*30*, *31*). Therefore, this experiment adopts randomization to select drivers, and multiple test data sets are compared with each other. In the experiment, the method of repeated measurement and cross-validation is adopted to achieve the purpose of repeated measurement, which ensures the reliability and validity of the data.

Data Analysis. To simplify the data processing flow, the temperature data is screened separately with the slope point as the feature point. The processed temperature data is compared with the original data, as shown in Figure 4. The inflection point of the measured temperature data of most sections, except for some sections, coincides with the height of the slope change point. The calibration of the subsequent model is studied with the filtered data.

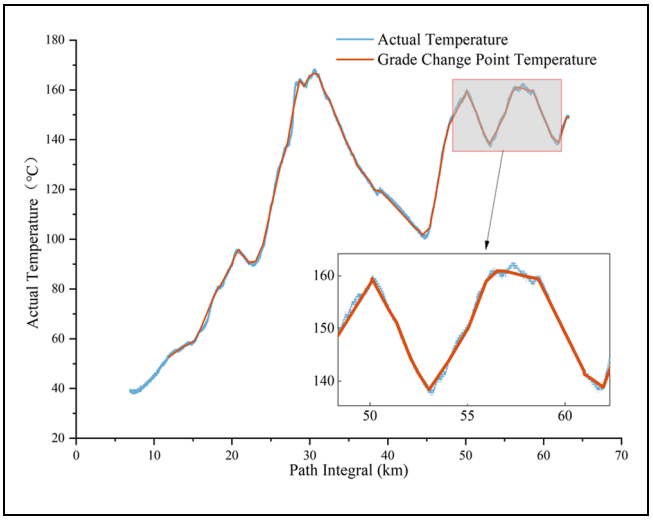

Figure 4. Comparison before and after data filtering.

According to the above theoretical model, the brake drum temperature value can be predicted by the given vehicle parameters, and the engine braking force can be obtained by substituting the calculation of Equation 13. The parameter calibration of the brake drum temperature rise model is related to the test section and vehicle selection of the real vehicle test. To make the brake drum temperature rise model more accurately predict the temperature value, it is necessary to combine the real vehicle test data to calibrate the brake drum temperature rise model. After calibrating the brake drum temperature rise model, the average difference between the predicted temperature and the actual vehicle temperature is about 5°C. It is considered that the temperature rise model can basically predict the braking temperature rise of the vehicle.

After calibrating the model, taking the continuous longitudinal slope of this section as the research object, the engine braking force is calculated and counted. The normal Q-Q diagram shows that the engine braking force

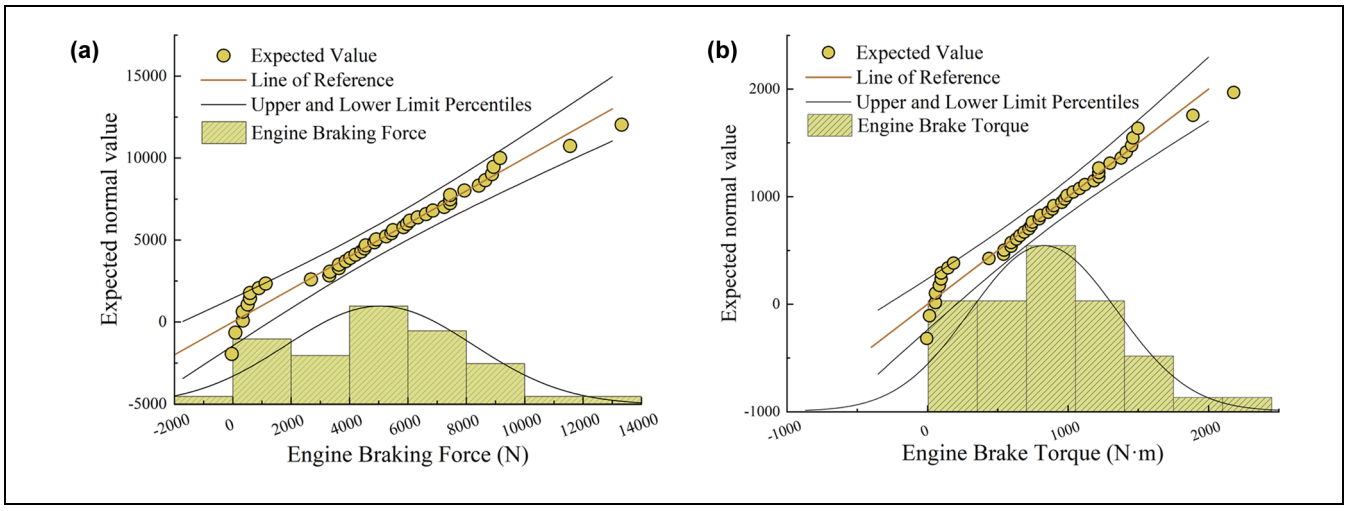

Figure 5. Normal distribution Q-Q diagram: (*a*) engine braking force Q-Q diagram and (*b*) engine braking torque Q-Q diagram.

Table 3. Simulation Test Condition Settings

Serial number	Controlling factor	Rated power (kW)	Weight (t)	Gear position	Speed (km/h)	Slope (%)
1	Power	300/330/400	49	12	60	−3
2	Weight	330	49/40/20	12	60	−3
3	Gear	330	49	12/11/10	60	−3
4	Speed	330	49	12	60/70/80/90	−3
5	Slope	330	49	12	60	−3/−5/−9/−12

distribution of each slope section is similar to the normal distribution, as shown in Figure 5. The braking force and braking torque are converted by Equation 14, in which the values of i_g, i_0, η_T, and r are determined according to the relevant parameters of the real vehicle test.

$$F_{eb} = \frac{T_{eb} i_g i_0 \eta_T}{r} \tag{14}$$

where

T_{eb} = the engine braking torque,
i_g = the transmission ratio of the gearbox,
i_0 = the transmission ratio of the main reducer (also known as the main transmission ratio), and
η_T = the mechanical efficiency of the transmission system.

The average value of engine braking torque is 824.5, and the variance is 523.2. The Q-Q diagram and distribution diagram of engine braking torque are drawn as shown in Figure 5. Because of the different values of multiple engine braking torques calculated on multiple slope sections, the mean value or other quantile value as the representative value of engine braking force needs to be determined. The simulation experiment can be used to study the influencing factors of engine braking performance, so as to select the representative value of truck engine braking torque more reasonably.

Simulation Experiment

Simulation Process

The vehicle dynamics simulation platform is used for further research to find out the influencing factors of engine braking performance, further study the engine braking performance under various power-to-weight ratio combinations, and verify the correctness of the engine braking performance calculated by the energy conservation mathematical model.

The simulation platform uses TruckSim, developed by the Mechanical Simulation Corporation, a professional automotive simulation software company in the U.S.

Table 3 presents the comprehensive simulation experiment parameters, with columns representing specific test parameters and rows indicating test series. The control factors were determined based on truck power-to-weight ratio and road longitudinal profiles, including engine power, vehicle weight, transmission gear, vehicle speed, and road slope. These parameters enable systematic

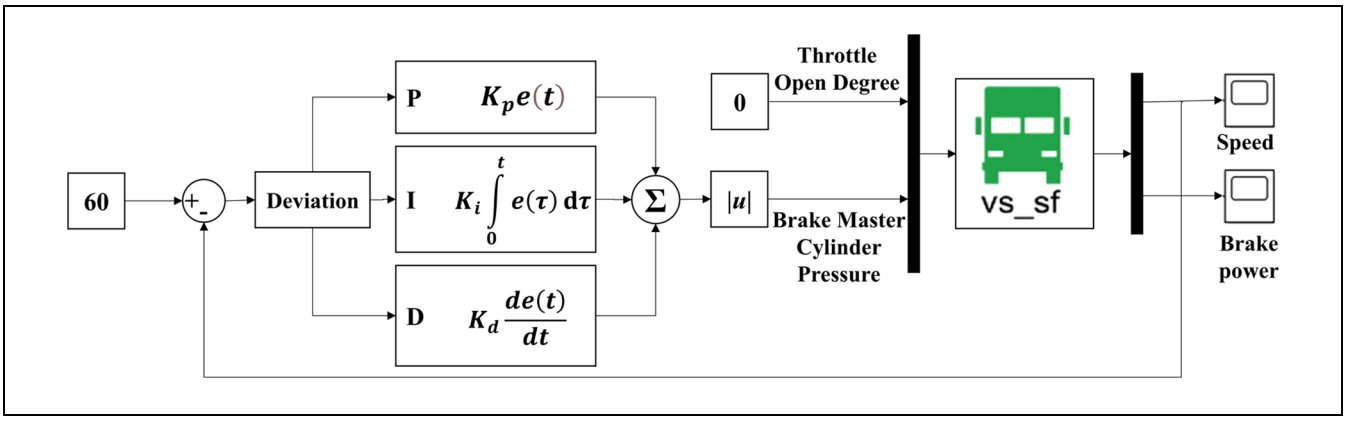

Figure 6. Simulink driving control.

Table 4. Summary of Kruskal–Wallis Test Results

Influencing factor	Level	*H*-statistic	*p*-value	Effect size (ε^2)	Significance
Speed	4	4,469.04	<0.001	0.932	Yes
Gear	3	3,185.81	<0.001	0.886	Yes
Power	3	3,138.45	<0.001	0.873	Yes
Slope	4	4.83	0.185	0.001	No
Weight	3	2.23	0.328	0.001	No

investigation of vehicle performance under various downhill driving conditions.

Parameter Setting

The simulation experiment is realized by the joint simulation of TruckSim and Simulink, and the corresponding parameters, such as road slope and vehicle gear, are set according to different research purposes, as shown in Figure 6.

Road and Vehicle Parameters. In the experiment, a 5 km straight asphalt road is used, with 0.85 friction coefficient and adjustable slope according to experiment requirements. Vehicle parameters were configured based on real vehicle test data from Table 2, while steering and suspension systems adopted default settings, as they were not primary research focuses.

Driver Parameters. Figure 6 illustrates the speed control system designed for continuous downhill driving. The system maintains zero throttle opening and employs proportional-integral-derivative (PID) control to dynamically adjust brake master cylinder pressure based on the difference between actual and target speeds, enabling uniform-speed downhill travel.

Simulation Data Analysis

Analysis of Influencing Factors. A series of simulation experiments based on Table 3 produced stable brake torque outputs. First, Shapiro-Wilk normality tests were performed on the data across different levels of each factor. The test results showed that data from all groups did not meet the normality assumption. Therefore, this study employed non-parametric testing methods—the Kruskal–Wallis test—to analyze the effects of various factors on the response variable.

Table 4 presents a summary of Kruskal–Wallis test results for the five factors. The test results demonstrate that three factors—speed, gear, and power—have significant effects on the response variable ($p < 0.001$), while the effects of the weight and slope factors are not significant ($p > 0.05$).

As far as effect sizes are concerned, the speed factor exhibited the largest effect size ($\varepsilon^2 = 0.932$), followed by gear ($\varepsilon^2 = 0.886$) and power ($\varepsilon^2 = 0.873$). All three factors demonstrated very large effect sizes, indicating strong influences on braking torque. In contrast, slope and weight showed effect sizes approaching zero,

Table 5. Descriptive Statistics for Significant Factors

Level	Mean	Median	SD	Min.	Max.
Speed (km/h)					
60	−63.60	−63.56	1.66	−85.53	−30.13
70	−83.31	−83.28	2.06	−110.31	−39.49
80	−103.03	−102.97	2.44	−135.02	−50.01
90	−122.74	−122.67	2.87	−161.01	−58.80
Gear					
10	−1,241.29	−1,241.53	30.18	−1,615.23	−539.46
11	−876.28	−876.67	20.13	−1,121.96	−402.84
12	−578.37	−578.67	12.46	−726.72	−288.05
Power (kW)					
300	−578.76	−578.40	15.07	−778.34	−274.19
330	−636.63	−636.24	16.29	−853.32	−303.19
400	−747.21	−746.82	18.52	−994.50	−358.53

Note: Max. = maximum; Min. = minimum; SD = standard deviation.

suggesting virtually no impact on braking torque. Table 5 presents descriptive statistics for the three significant factors across different levels.

Analysis by Tables 4 and 5

- In the parameter of power-to-weight ratio, the main factor affecting the engine's braking performance is its power, while the truck's weight has little effect.
- Engine braking torque exhibits an inverse relationship with gear selection; it decreases when shifting to higher gears. Conversely, engine braking torque increases as vehicle speed rises. Consequently, the engine braking characteristics of the truck vary significantly across different gears and speeds.
- The engine braking torque distribution of trucks running on different slopes is not significantly different and remains at the same level, indicating that the slope has little effect on the engine braking performance.

In summary, rated power, vehicle speed, and gear selection significantly influence engine braking performance, necessitating further quantitative investigation of these factors.

Braking Torque Modeling. According to vehicle dynamics principles, vehicle speed, transmission gear ratio, and engine speed are mathematically correlated by Equation 15.

$$V = 0.377\frac{rn}{i_g i_0} \tag{15}$$

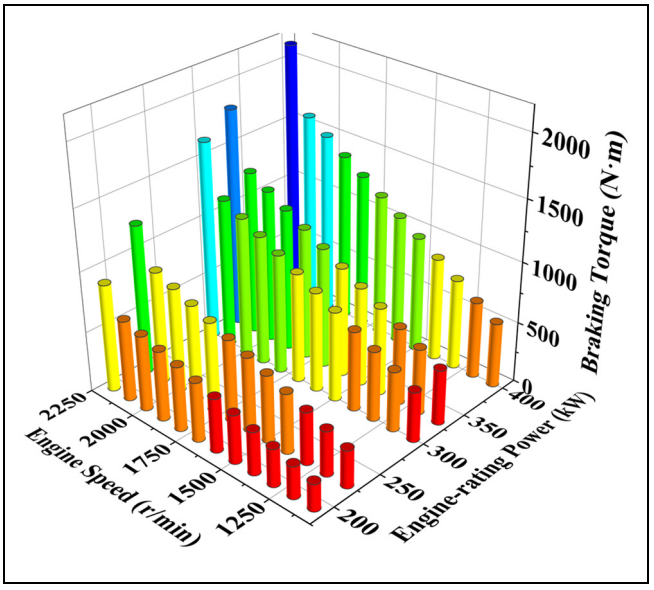

Figure 7. Power and braking torque at various engine speeds.
Note: The color mapping indicates the magnitude of braking torques in different ranges.

where

V = the vehicle speed (km/h),
r = the tire radius (m),
n = the engine speed (rpm),
i_g = the transmission ratio of the gearbox, and
i_0 = the main transmission ratio.

Analysis of this relationship reveals that, at a constant vehicle speed, a higher gear transmission ratio (lower gear) results in higher engine speed; similarly, at a constant gear position, higher vehicle speed leads to higher engine speed. This relationship demonstrates the direct influence of vehicle speed and gear selection on engine operating conditions. Further analysis indicates that vehicle speed and gear position affect engine braking performance through a common mechanism. Whether changing vehicle speed or shifting gears, the fundamental cause of their influence on engine braking performance lies in the alteration of engine speed. Thus, the present research conducts a further investigation into engine braking torque across different power levels and engine speeds.

Through the 190 kW, 220 kW, 300 kW, and 330 kW engine models in TruckSim, the relationship between power and braking torque at each engine speed is derived and logarithmically fitted, as shown in Figure 7.
The fitting results of the experiment model at the engine speed of 1,100–2,200 r/min are shown in Table 6.

The relationship between the engine speed and the braking torque during the braking process of the engine with a rated power of 400 kW is $T = 1.0702n - 644.49$.

Table 6. Logarithmic Fitting of Power and Braking Torque at Various Engine Speeds

Engine speed (r/min)	Logarithmic fitting equation	R^2
1,100	$T = -409.2\ln(P) + 1{,}916.8$	0.9971
1,200	$T = -484.3\ln(P) + 2{,}263.6$	0.9968
1,300	$T = -570.9\ln(P) + 2{,}673.2$	0.9970
1,400	$T = -653.4\ln(P) + 3{,}060.2$	0.9971
1,500	$T = -733.8\ln(P) + 3{,}435.4$	0.9970
1,600	$T = -815.8\ln(P) + 3{,}819.4$	0.9970
1,700	$T = -898.3\ln(P) + 4{,}206.4$	0.9970
1,800	$T = -979.6\ln(P) + 4{,}587$	0.9970
1,900	$T = -1{,}060\ln(P) + 4{,}965$	0.9971
2,000	$T = -1{,}144\ln(P) + 5{,}355.7$	0.9970
2,100	$T = -1{,}225\ln(P) + 5{,}733.7$	0.9970
2,200	$T = -1{,}630\ln(P) + 7{,}632.8$	0.9970

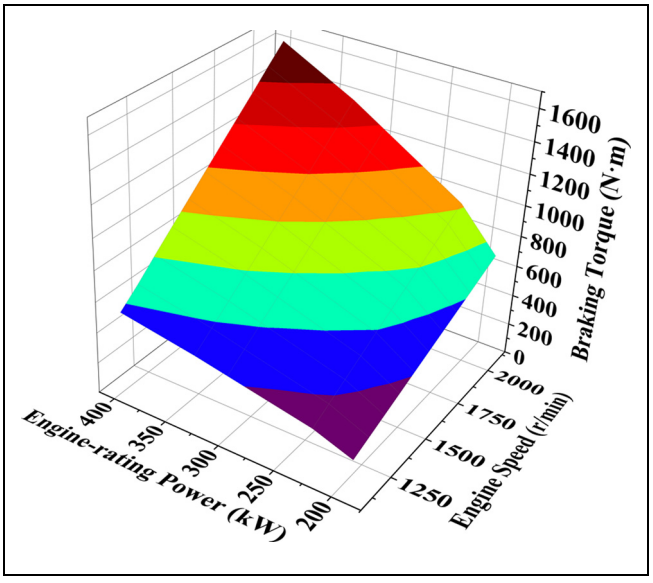

Figure 8. Relationship between engine speed and braking torque under different rated powers.
Note: The color mapping indicates the magnitude of braking torques in different ranges.

The mathematical model of engine speed and braking torque under any engine power can be obtained from Table 6. Figure 8 presents the relationship between engine speed and braking torque for engine power ranging from 190 kW to 400 kW.

Analysis by Figure 8. The relationship between engine braking torque and operational parameters reveals distinct patterns. Under constant power conditions, engine braking torque increases proportionally with engine speed. This relationship, as expressed in Equation 15, indicates that lower gear selections generate greater braking torque because of the mechanical advantage provided by the transmission ratio. Additionally, when comparing engines operating at identical speeds, those with higher power ratings demonstrate superior braking performance, suggesting that engine displacement and design characteristics significantly influence braking capacity.

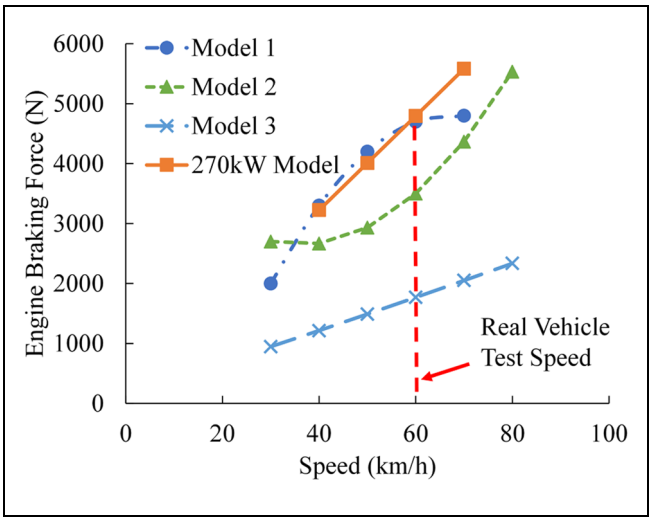

Figure 9. Different engine braking force models.

Table 7. Experiment Parameters of Each Model

Model category	Engine model	Engine rated power (kW)
Model 1 (*32*)	CA6DM235E3	270
Model 2 (*33*)	DRL4251A9	230–250
Model 3 (*34*)	YC6G270-20	199
270 kW model	NA	270

NA = not available.

Model Verification. From the above analysis, it can be seen that the engine braking performance is related to the engine speed and engine power. Therefore, based on the theoretical model calculations presented in Theoretical Model Construction, this study conducted mean value processing of the engine braking forces under different gradients, which served as the representative value of the total vehicle braking force during constant-speed downhill operation. The engine braking torque data under 400 kW power conditions was obtained through computational analysis. Comparative verification showed that the relative error between the simulation results and mathematical model calculations was 5.84%.

To further verify whether the engine braking performance calculated by the model is reliable, the engine calculation model proposed by the relevant literature is used to calculate and compare with the results of the model in this study at 270 kW. The calculation results

Table 8. Reasonable Reduction Speed of Heavy-Duty Trucks

Design speed (km/h)	120	100	80	60
Average velocity of slope bottom	80	75	70	55
Minimum allowable speed	60	55	50	40
Velocity change value	20	20	20	15

are shown in Figure 9. The experiment vehicle or engine models of each model and the corresponding engine power are listed in Table 7.

It can be seen from Figure 9 that the braking force model of different rated power engines has the following rules through analysis:

- From the overall trend analysis, the engine braking force exhibits a significant positive correlation with vehicle speed. Further analysis of Table 6 data demonstrates that, under identical speed conditions, a distinct positive correlation exists between engine rated power and braking force output, indicating that higher rated power corresponds to proportionally greater braking force generation.
- Comparing the derived model with the literature model, the engine braking force calculated by the 270 kW model is in good agreement with the calculation results of Model 1 with the same power in the 40–60 km/h range. After calculation and comparison, the engine braking force error is 6.96% at 60 km/h, the engine braking force error is 9.41% at 50 km/h, and the engine braking force error is 7.3% at 40 km/h, indicating acceptable accuracy within this range. Therefore, the model is considered valid within the 40–60 km/h speed range. Its accuracy outside this range has not been validated.
- From the perspective of the trend of predictive braking force, there are linear and nonlinear models. In Model 1, the engine braking force increases linearly in the range of 20–50 km/h, and the engine braking force gradually tends to be gentler with the increase of vehicle speed. Model 2 shows a linear increase in engine braking force in the range of 60–80 km/h, and the upward trend of engine braking force increases with the increase of vehicle speed. In Model 3, the engine braking force increases linearly with the increase in vehicle speed.

Determination of Critical Slope Length

Theoretical Analysis of Average Longitudinal Slope

The *Highway Route Design Specification* (JTG D20-2017) points out that, when the average continuous long and steep downhill slope is less than 2.5%, the slope length is not limited. The continuous slope length is limited when the average longitudinal slope is greater than 2.5%. However, the average longitudinal slope of the whole section may occur without limiting the length of the continuous slope, and the average longitudinal slope of the interval may occur by limiting the length of the continuous slope. Therefore, it is necessary to study the critical slope length under the reasonable average longitudinal slope.

The critical length of the longitudinal slope of the downhill is usually determined by the deceleration of the truck during the downhill process. The braking performance of vehicles with different slopes and different performances is significantly different. The minimum speed of the vehicle should be 50%–60% of the design speed, or the speed difference between the adjacent road sections is 15–20 km/h. Table 8 shows the reasonable reduction speed of heavy vehicles at different design speeds (*35*). According to the different rated power of the truck under certain deceleration conditions, the relationship between vehicle speed and slope length can be obtained, and this can be used as a reference for setting the location of the refuge lane. The relationship curve between speed reduction and slope length can be used to determine the critical slope length under different power-to-weight ratios. In this paper, the relationship between the speed and the slope length of the truck with a power-to-weight ratio of 5–8 kW in the longitudinal slope of 1%–12% is further studied.

Calculation of Critical Slope Length

Assuming vehicles with different power-to-weight ratios are descending within a specified slope range under engine braking conditions only, the vehicles are primarily subjected to the combined effects of air resistance, rolling resistance, and engine braking force. By establishing vehicle dynamics equations to solve for instantaneous acceleration and applying differential equation theory, the variation patterns of travel distance and speed for vehicles with different power-to-weight ratios under varying slope conditions can be derived, as specifically shown in Equations 16, 17, and 18.

$$mg\sin\theta - F_w - F_f - F_{eb} = ma \tag{16}$$

$$x = \int_{V_1}^{V_2} \frac{V}{a} dV \tag{17}$$

$$x = \int_{V_1}^{V_2} \frac{2mV}{2mg(\sin\theta - f\cos\theta) - C\rho SV^2 - 2F_{eb}} dV \tag{18}$$

where

x = the distance (m),

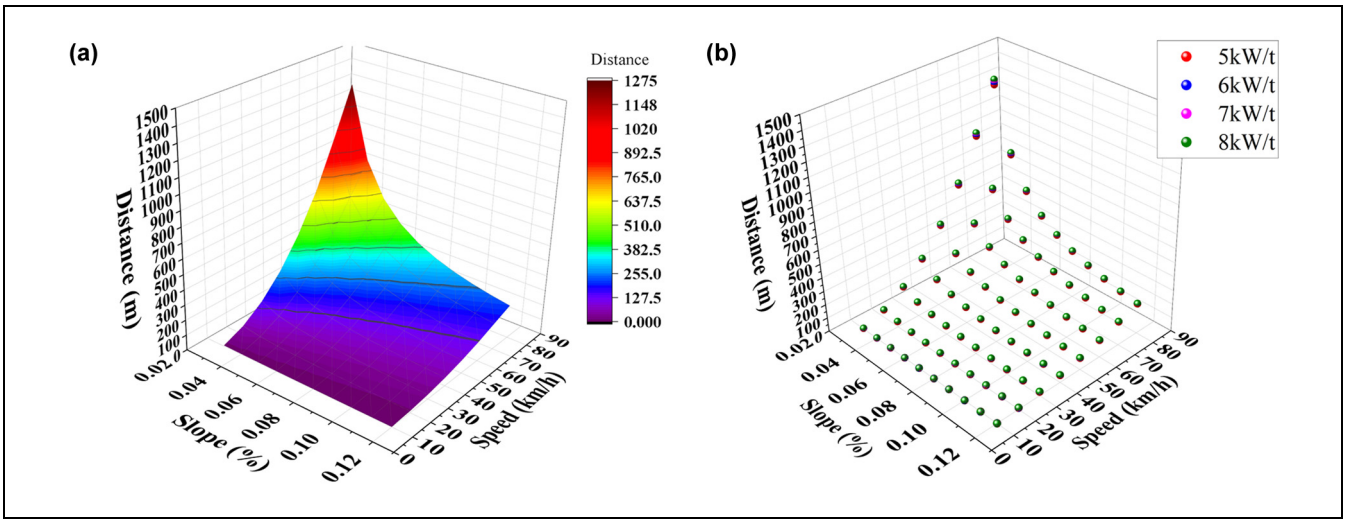

Figure 10. 3D surfaces and scatter plots: (*a*) 3D surface map with color mapping and (*b*) 3D scatter plot.

V_1 = the initial speed (m/s),
V_2 = the final speed (m/s),
m = the vehicle mass (kg), and
θ = the design slope of the longitudinal slope.

Select 5–8 kW/t power-to-weight ratio as the analysis range, set the engine rated power of 245, 294, 343, and 392 kW, load capacity of 49 tons, corresponding to 5, 6, 7, and 8 kW/t power-to-weight ratio of the truck; according to Equation 18, the speed change curve of the truck with different power-to-weight ratios on the 1%–12% longitudinal slope can be calculated. To further establish the distance-speed-slope model of the truck downhill under the power-to-weight ratio of 5–8 kW/t, a 3D surface map with color mapping and a 3D scatter plot are drawn (see Figure 10).

Through the analysis of the slope value with the power-to-weight ratio of 5–8 kW/t, it is found that the trend of the curve is consistent. The calculation results of the power-to-weight ratio of 5 kW/t on the slope of 1%–5% are selected as an example for analysis. It can be seen that the increase in the speed of the truck tends to be gentle during the downhill process, and the truck as a whole reaches a stable operating state. When the slope is greater than 3%, the downhill speed of the truck relying solely on the engine brake will reach a degree that is difficult to control.

To explore the influence of power-to-weight ratio on the speed change of trucks during the downhill process, the speed and distance changes of trucks with different power-to-weight ratios on the same slope value are analyzed. The analysis of the slope value of 1%–12% shows that the curve trend is consistent. Here, the slope value of 1% is selected as an example to analyze the curve trend. Under specific slope conditions, the rated power of trucks exhibits a significant negative correlation with their speed variation trend: the higher the rated power, the slower the speed increase rate, and the lower the corresponding steady-state speed value. This indicates that trucks with a higher power-to-weight ratio experience a more gradual speed increase when relying solely on engine braking during downhill descent.

Consequently, it can be concluded that the power-to-weight ratio of trucks is positively correlated with their braking performance. The higher the power-to-weight ratio, the better the speed control capability during long downhill descents, resulting in smoother speed variations and significantly enhanced downhill driving safety.

The polynomial is used to fit the four surfaces drawn, and the polynomial form is shown in Equation 19.

$$f(i, V) = P_{00} + P_{10}x + P_{01}y + P_{20}x^2 + P_{11}xy \quad (19)$$

The calculation model of the downhill slope length of the truck under a specific power-to-weight ratio can be obtained by fitting, as shown in Figure 11*a*. The relationship between the speed and distance of the 5–8 kW/t truck on a specific slope can be calculated by this model. Figure 11*b* is the residual error of the model fitting. It can be seen that the prediction effect of the model is poor near the slope of 0.03, and the residual error is more than 100. As presented in Table 9, the polynomial fitting coefficients and goodness-of-fit are listed, with all R^2 values exceeding 0.9, indicating that the model demonstrates satisfactory fitting performance.

Discussion

The mathematical model of engine braking performance based on energy conservation constructed in this study demonstrates significant practical value for

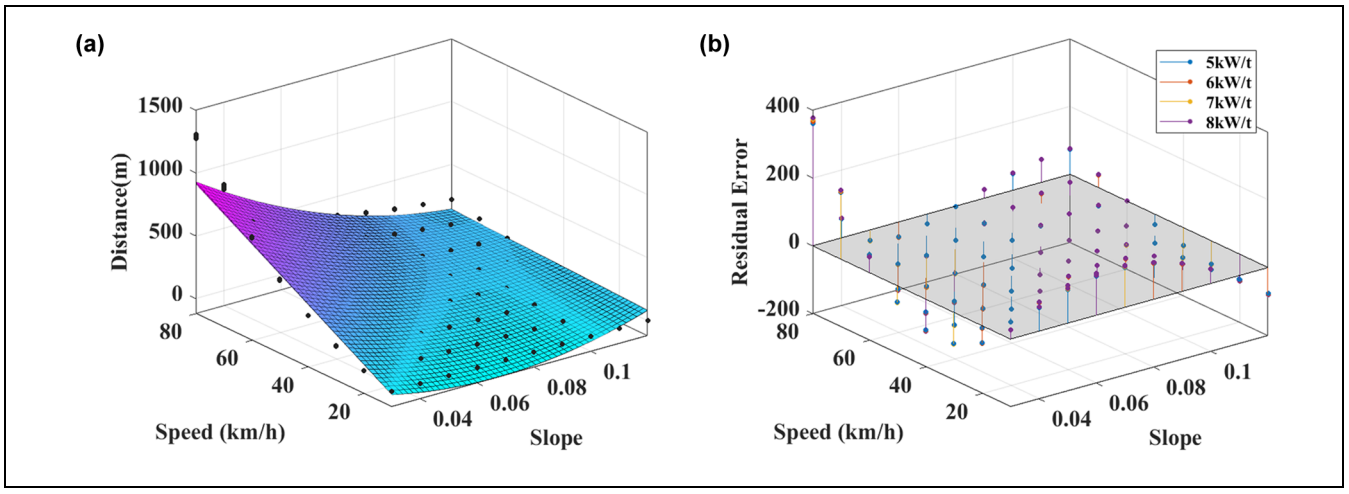

Figure 11. Truck downhill distance-speed-slope model (5–8 kW/t): (*a*) fitting picture and (*b*) residual plot.

Table 9. Model Fitting Parameters

Fitted model	P_{00}	P_{10}	P_{01}	P_{20}	P_{11}	R^2	RMSE
5 kW/t	15.7333	−7.81E + 03	17.5105	6.87E + 04	−137.8414	0.9042	72.362
6 kW/t	16.9578	−7.91E + 03	17.6511	6.96E + 04	−139.2092	0.9030	73.388
7 kW/t	18.0144	−8.00E + 03	17.7718	7.04E + 04	−140.3845	0.9020	74.276
8 kW/t	18.9461	−8.08E + 03	17.8782	7.10E + 04	−141.4217	0.9011	75.064

Note: RMSE = root mean square error.

understanding truck downhill dynamics. Through theoretical model construction, experiment verification, and engineering application, our three-step approach has successfully established a comprehensive framework for analyzing speed and driving distance characteristics of trucks relying on engine braking in continuous, long, downhill scenarios.

The simulation results reveal that the power-to-weight ratio of the truck and engine speed significantly affect the engine braking torque during the downhill process. The developed distance-speed prediction model for vehicles with power-to-weight ratios ranging from 5 to 8 kW/t on longitudinal slopes of 1% to 12% demonstrates high goodness-of-fit ($R^2 > 0.9$), with an average error of 7.83% in the speed range of 40–60 km/h. This indicates that the energy conservation model can reliably predict engine braking performance under most operating conditions, although larger residuals were observed in gentle slope regions.

Our findings indicate a positive correlation between a truck's power-to-weight ratio and its engine braking performance, with higher ratios corresponding to enhanced speed control capability during long downhill descents. While the research focuses on the relationship between power-to-weight ratios and braking performance, the practical implementation of safety measures involves additional controllable factors (*36*). Road designers can select appropriate speed limits to post along routes, and drivers can choose both the speed and gear selection when descending grades. In this context, our model results can inform the posting of appropriate descent speed limits and support signs advising truck drivers to use the lowest gear possible, which are key strategies for reducing instances of overheated brakes on long downgrades.

Furthermore, the distance-speed model established for trucks with different power-to-weight ratios provides valuable decision-making support for both design and operational phases. During the design stage, it can effectively evaluate and compare the safety of different schemes, helping to optimize design layouts. During operations, it can inform highway safety measures, ensuring trucks operate safely under complex road conditions.

Despite these promising results, several aspects warrant further investigation to enhance the model's robustness and applicability. The mathematical model established in this study has been verified to be accurate under certain conditions, but there remains room for further optimization. The current speed-distance

relationships are primarily derived from simulation analysis, and future field validation under controlled conditions would strengthen the model's reliability. Additionally, future research could introduce more influencing factors, extend the framework to other vehicle types and different road conditions, or explore the synergy between road safety measures and vehicle braking performance to broaden the model's application scope.

Conclusions

This study explored the application of energy conservation principles in predicting the engine braking performance of trucks on continuous downhill sections. A mathematical model was developed for this specific scenario, and its prediction accuracy was validated under certain conditions. Using simulation experiment results, we analyzed the correlation between the vehicle's power-to-weight ratio and braking effectiveness, confirming a positive relationship between them. Furthermore, we derived a distance-speed model for trucks with a power-to-weight ratio of 5–8 kW/t under longitudinal gradients of 1%–12%.

In this research, we focused on practical validation of the model under limited conditions and discussed the potential value of the findings for highway safety engineering. We hope these results can provide a reference for enriching the analytical methods of truck braking performance and offer modest methodological support for relevant engineering practices.

Author Contributions

The authors confirm contribution to the paper as follows: study conception and design: D. Wei, C. Zhang, B. Wang; data collection: C. Zhang, Y. Gao, T. Guo; analysis and interpretation of results: D. Wei, Y. Gao; draft manuscript preparation: D. Wei, C. Zhang, Y. Gao, T. Guo, B. Wang. All authors reviewed the results and approved the final version of the manuscript.

Declaration of Conflicting Interests

The authors declared no potential conflicts of interest with respect to the research, authorship, and/or publication of this article.

Funding

The authors disclosed receipt of the following financial support for the research, authorship, and/or publication of this article: This research was supported by the National Key Research & Development Program of China (Grant Nos. 2021YFB2600103, 2020YFC1512005, 2021YFB2301602; the National Natural Science Foundation of China (Grant No. 72371036); and the Science and Technology Project of Sichuan Transportation Department (Grant Nos. 2021-ZL-15, 2022-ZL-04, and 2023-A-04.

ORCID iDs

Dibin Wei https://orcid.org/0009-0001-4081-8443
Chi Zhang https://orcid.org/0000-0003-0713-3722
Yanyang Gao https://orcid.org/0009-0001-5818-6106
Tingyu Guo https://orcid.org/0009-0000-5159-226X
Bo Wang https://orcid.org/0000-0002-0593-6612

References

1. PRC Ministry of Transport. *Statistical Bulletin on Transportation Sector Development in 2023*. June 2024.
2. Chinese Academy of Science. *Report on Mountain Research and Mountain Development in China*. A Series of Research Reports on Resources and Environment, November 2022.
3. Xie, S., X. Ji, W. Yang, and C. Hu. Analysis of Traffic Accident Characteristic and Difference in Two-Lane Plateau Mountain Highways. In *CICTP 2020*, pp. 4408–4419. Available at: https://ascelibrary.org/doi/abs/10.1061/9780784482933.378.
4. Zhao, Y., J. Li, and X. Ying. Study on Risk of Long-Steep Downgrade Sections of Expressways Based on a Fuzzy Hierarchy Comprehensive Evaluation. *Applied Sciences*, Vol. 12, No. 12, 2022, p. 5924.
5. Zheng, Y., G. Huiji, and X. Wei. The Evaluation Analysis of Design Code About the Road Design of Longitudinal Gradient in the Mountain Road. 2017.
6. Archilla, R., and J. Morrall. Traffic Characteristics on Two-Lane Highway Downgrades. *Transportation Research Part A: Policy and Practice*, Vol. 30, No. 2, 1996, pp. 119–133.
7. Meier, H. Hydrodynamische Dauerbremsachse für Anhänger und Sattelauflieger. *Automobiltechnische Zeitschrift*, Vol. 75, No. 9, 1973, pp. 314–319.
8. Rahmani, O., I. Aghayan, A. S. Abdollahzadeh Nasiri, M. Kane, and F. Hadadi. A Nonlinear Analytical Approach for Estimating Vehicle Braking Distance Based on Multi-Body Dynamic Simulation. *Sādhanā*, Vol. 49, No. 1, 2024, p. 20.
9. Abdi Kordani, A., O. Rahmani, A. S. Abdollahzadeh Nasiri, and S. M. Boroomandrad. Effect of Adverse Weather Conditions on Vehicle Braking Distance of Highways. *Civil Engineering Journal*, Vol. 4, No. 1, 2018, pp. 46–57.
10. Bowman, B. L., and I. Goodell-Grivas, and U.S. Federal Highway Administration, Office of Safety and Traffic Operations Research and Development. *Grade Severity Rating System (GSRS): User's Manual*. U.S. Department of Transportation, Federal Highway Administration, Research, Development, and Technology, 1990.
11. Coleman, M. *Use of Auxiliary Brakes in Heavy Vehicles*. Austroads, 2014.
12. He, Y., E. He, L. Zhang, J. Gao, C. Yang, L. Sun, et al. Brake Drum Temperature Rise and Its Influence on Truck

Driving Safety in Tunnel Groups Section. *Complexity*, Vol. 2024, No. 1, 2024, p. 5552467.
13. Umaras, E., A. Barari, and M. S. G. Tsuzuki. Heavy Vehicles Brake Drums—An Accurate Evaluation on Thermal Loads in Severe Service Conditions. *International Journal of Automotive Technology*, Vol. 22, No. 2, 2021, pp. 371–382.
14. Arkatkar, S. S., and V. T. Arasan. Effect of Gradient and Its Length on Performance of Vehicles under Heterogeneous Traffic Conditions. *Journal of Transportation Engineering*, Vol. 136, No. 12, 2010, pp. 1120–1136.
15. Yuchuan, D., Y. Lei, and S. Luo. Optimization of Combined Horizontal and Vertical Curves Design of Mountain Road Based on Vehicle–Road Coordination Model. In *2019 5th International Conference on Transportation Information and Safety (ICTIS)*, IEEE, 2019, pp. 16–24.
16. Wang, F., J. Wang, X. Zhang, D. Gu, Y. Yang, and H. Zhu. Analysis of the Causes of Traffic Accidents and Identification of Accident-Prone Points in Long Downhill Tunnel of Mountain Expressways Based on Data Mining. *Sustainability*, Vol. 14, No. 14, 2022, p. 8460.
17. Yu, B. Modeling Truck Motion along Grade Sections. 2005.
18. Gillespie, T. D. Methods for Predicting Truck Speed Loss on Grades: Final Technical Report. 1985.
19. Lan, C. J., and M. Menendez. Truck Speed Profile Models for Critical Length of Grade. *Journal of Transportation Engineering*, Vol. 129, No. 4, 2003, pp. 408–419.
20. Rakha, H., I. Lucic, S. H. Demarchi, J. R. Setti, and M. V. Aerde. Vehicle Dynamics Model for Predicting Maximum Truck Acceleration Levels. *Journal of Transportation Engineering*, Vol. 127, No. 5, 2001, pp. 418–425.
21. Zhao, L., X. Zhang, Y. Zhang, and T. Xu. Length of Slope Determination with Heavy Duty Vehicles. In H. Wang, H. Wei, L. Zhang, and Y. An (eds.), *Proceedings of Chang'an University*, 2020, pp. 4255–4267.
22. Bokare, P. S., and A. K. Maurya. Acceleration and Deceleration Behaviour of Truck on Indian Highway. *Indian Highways*, Vol. 42, 2014, p. 74.
23. Castillo-Manzano, J. I., M. Castro-Nuño, and X. Fageda. Exploring the Relationship Between Truck Load Capacity and Traffic Accidents in the European Union. *Transportation Research Part E: Logistics and Transportation Review*, Vol. 88, 2016, pp. 94–109.
24. Li, W. L., W. J. Zhou, L. X. Gao, and Y. Chen. Real-Time Monitoring for Vehicle Brake Temperature Rise in Continuous Long Downhill. *Applied Mechanics and Materials*, Vols. 300–301, 2013, pp. 916–919.
25. Yu, Q., Y. Chen, J. Ma, R. Guo, and Q. Zhang. Affect of Engine Brake and Exhaust Brake on Bus Brake Stability. *Journal of Traffic and Transportation Engineering*, Vol. 3, No. 3, 2003, pp. 64–67.
26. Umaras, E., A. Barari, and M. S. G. Tsuzuki. Heavy Vehicles Brake Drums—An Accurate Evaluation on Thermal Loads in Severe Service Conditions. *International Journal of Automotive Technology*, Vol. 22, No. 2, 2021, pp. 371–382.
27. Zhao, X., Q. Yu, X. Yuan, and P. Shi. A Research on the Brake Temperature Rise Model of Heavy Truck Running on Long Downhill. *Automotive Engineering*, Vol. 37, No. 4, 2015, pp. 472–475.
28. Zhang, C., Y. Hou, K. Yang, J. Qin, and H. Zhang. Review of Brake Drum Temperature Rise Model for Vehicle on Long and Steep Downgrades of Highway. *Journal of Chang'an University,* Vol. 39, No. 3, 2019, pp. 96–107.
29. Zhang, C., Y. Hou, J. Qin, and H. Zhang. Safety Design Method of Long Slope Downhill Slope Based on Temperature Increase of Brake Drum. *Journal of South China University of Technology (Natural Science Edition)*, Vol. 47, No. 10, 2019, pp. 139–150.
30. Chen, L., and Z. Guo. Prediction Model of Brake Drum Temperature on Continuous Downgrade Segments in High-Altitude Environment. *Journal of Beijing University of Technology*, Vol. 46, No. 7, 2020, pp. 772–781.
31. Han, Y., J. Xu, Y. Liu, G. Liu, and H. Yang. Safety Grade Length for Driving at Long-Steep Downgrade Highway. *Journal of Chang'an University*, Vol. 30, No. 5, 2010, pp. 35–39.
32. Li, C., F. Li, and C. Wang. Test Research on Auxiliary Braking Performances of Large Freight Vehicles. *Journal of University of Jinan (Science and Technology)*, Vol. 37, No. 6, 2023, pp. 758–765.
33. Jin, E., and B. Du. Prediction Model of Brake Temperature of Truck on Long and Steep Downgrade. *Journal of Highway and Transportation Research and Development*, Vol. 28, No. 2, 2011, pp. 133–136.
34. Zhao, X., X. Yuan, and Q. Yu. A Critical Study of Driving Performance of Heavy-Duty Vehicle Running on Long Downhill Road Using Engine Brake. *The Open Mechanical Engineering Journal*, Vol. 8, 2014, pp. 475–479.
35. Xu, T., L. Zhao, M. Zhang, M. Li, and J. Liu. Critical Length Determination for Long and Longitudinal Slope of Expressway Based on Performance of Heavy-Duty Vehicles. *Journal of Chang'an University (Natural Science Edition)*, Vol. 39, No. 3, 2019, pp. 108–116.
36. Moomen, M., M. Rezapour, and K. Ksaibati. An Investigation of Influential Factors of Downgrade Truck Crashes: A Logistic Regression Approach. *Journal of Traffic and Transportation Engineering*, Vol. 6, No. 2, 2019, pp. 185–195.